

# PCCP

Accepted Manuscript



This is an *Accepted Manuscript*, which has been through the Royal Society of Chemistry peer review process and has been accepted for publication.

*Accepted Manuscripts* are published online shortly after acceptance, before technical editing, formatting and proof reading. Using this free service, authors can make their results available to the community, in citable form, before we publish the edited article. We will replace this *Accepted Manuscript* with the edited and formatted *Advance Article* as soon as it is available.

You can find more information about *Accepted Manuscripts* in the [Information for Authors](#).

Please note that technical editing may introduce minor changes to the text and/or graphics, which may alter content. The journal's standard [Terms & Conditions](#) and the [Ethical guidelines](#) still apply. In no event shall the Royal Society of Chemistry be held responsible for any errors or omissions in this *Accepted Manuscript* or any consequences arising from the use of any information it contains.

## Self-assembly of SnO<sub>2</sub> quantum dots into hierarchically ordered structure assisted by oriented attachment

Cite this: DOI: 10.1039/x0xx00000x

Zanyong Zhuang,<sup>a</sup> Xiaogang Xue<sup>a</sup> and Zhang Lin<sup>a\*</sup>

Received 00th January 2012,

Accepted 00th January 2012

DOI: 10.1039/x0xx00000x

www.rsc.org/

**Taking SnO<sub>2</sub> quantum dots with random orientation as precursor, NaOH induces self-assembly of SnO<sub>2</sub> dots to form the nanowires, side-by-side attachment of which generates hierarchically ordered structures. The multistep oriented attachment mechanism can help to describe the oriented assembly of big nanocrystals.**

In-depth understanding of the factors that affect particles-mediated (non-classical) crystallization pathways, is one of the keys to achieve a fine control over the bio-inspired syntheses of hierarchically ordered nanostructures (e.g. CaCO<sub>3</sub>).<sup>1-5</sup> So far, a growing body of researches have demonstrated that, the particles-mediated growth pathways prove closely related to the size, surface capping and aggregation state of nanocrystals.<sup>2, 3, 5</sup> For instance, the growth rate of nanocrystals via oriented attachment (OA) mechanism is normally dependent on the size and surface capping of nanocrystals.<sup>3, 6-8</sup> Capping agents, sometimes, induce a precise arrangement of nanocrystals as building blocks, resulting in mesocrystals formation.<sup>5, 9, 10</sup> Additionally, aggregation state of nanocrystals which helps to reduce the interparticles distance, probably, triggers the growth of adjacent nanocrystals.<sup>2, 4, 11, 12</sup> However, how these factors coordinately control the particles-mediated crystal growths thus to achieve hierarchical nanostructures formation, is still poorly defined.

Tailoring the size and shape of tin oxide (SnO<sub>2</sub>) crystal is of great interest for its wide applications in areas of lithium-ion batteries, gas sensors, and sensitized solar cells.<sup>13, 14</sup> Several studies have indicated that, nano-SnO<sub>2</sub> with low solubility in water normally grow via particles attachment.<sup>8, 15</sup> As demonstrated in our previous works, SnO<sub>2</sub> (2 nm) quantum dots (QDs) coarsened in water at 250 °C can fast grow to a limiting size about twice of that of primary nanoparticles (4-5 nm).<sup>7</sup> However, with the increasing of particle size is a fast slowing down of the growth rate of SnO<sub>2</sub>. The growth of SnO<sub>2</sub> QDs with size over 4-5 nm is essentially ceased.<sup>7</sup> Restart of crystal growth requires continuous coarsening treatment of samples over 100 hours, till the aggregation degree of nanocrystals increase to a critical value.<sup>16</sup> After that, the aggregate of SnO<sub>2</sub> nanocrystals will fast grow into one single crystal, wherein the particle size jumps directly from ~ 4 to 350 nm.<sup>16</sup> What should be noted is that, the bulk-like crystals do not show any preferred orientation.<sup>7, 16</sup>

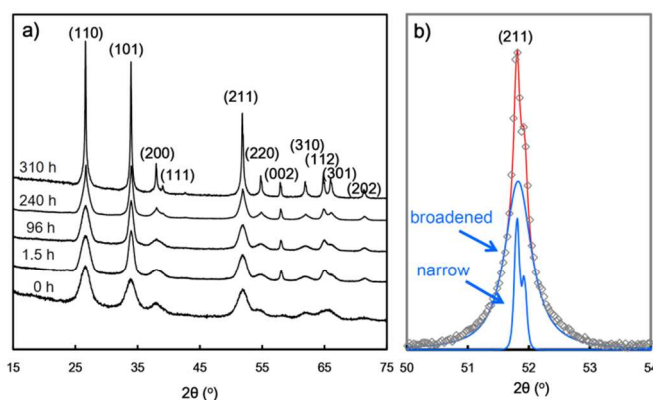


**Fig. 1** a) XRD patterns of SnO<sub>2</sub> (4-5 nm) coarsened in 1.2 M NaOH for 0, 1.5, 96, 240, and 310 h, respectively, b) Gauss fitting of (211) diffraction peak (red line) of SnO<sub>2</sub> treated for 310 h by a pair of broadened and narrow (blue line) peaks, which indicates the coexistence of big SnO<sub>2</sub> crystals and small nanocrystals. No phase transformation occurred.

Now the idea in this work was to find out, how surface modification influences the crystal growth behavior. To check this, immediately after nanocrystals grew to a limited size of 4-5 nm in water, NaOH was added into the coarsening system, considering that a presence of OH<sup>-</sup> possibly could facilitate particles interaction, and open access to attachment and assembly of adjacent nanocrystals.<sup>17, 18</sup> Additionally, changing the pH value in synthetic works, sometimes, generated SnO<sub>2</sub> nanocrystals with anisotropic shapes, e.g. nanowires.<sup>19, 20</sup> Investigation of the influence of surface modification on tailoring insoluble nanocrystals growth, might help to build novel nanomaterials, e.g. hierarchically ordered nanostructures.

In this work, the growth of SnO<sub>2</sub> restarted right after an addition of NaOH (1.2 M). Moreover, the SnO<sub>2</sub> QDs can spontaneously assemble to form one-dimensional (1-D) nanowires, side-by-side attachment and coalescence of which fabricated 3-D hierarchically ordered structures. Multistep OA mechanism can help to describe the oriented assembly of big nanocrystals, wherein a presence of OH<sup>-</sup> could help to induce aggregation, reduce energy barrier, and bridge the OA-like growth of adjacent nanocrystals.

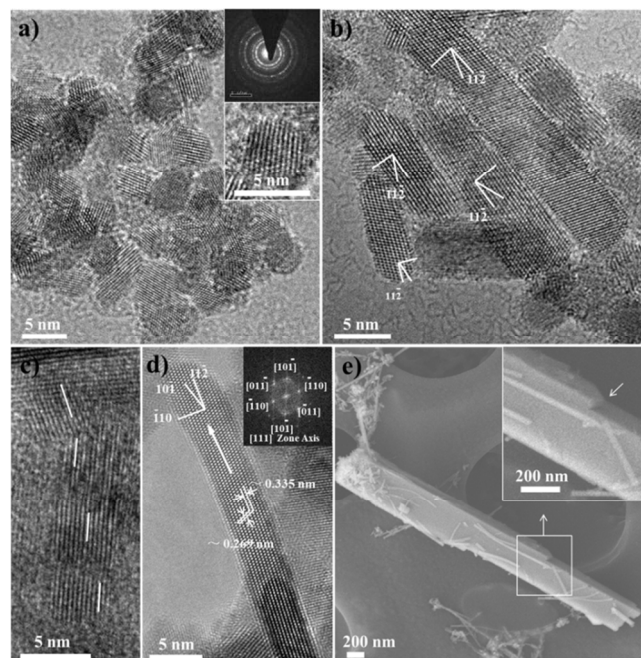


**Fig.2** Microscopic images of SnO<sub>2</sub> coarsened in 1.2 M NaOH at 250 °C. TEM image of a) QDs with random orientation at 0 h, and b) coexistence of QDs and nanorods growing along [11-2] direction at 1.5 h. c) growth trace suggesting QDs with common crystallographic orientation attached into nanowire at 1.5 h. d) SnO<sub>2</sub> nanowire showing preferential growth along [11-2] direction at 24 h, and e) SEM image of a big elongated SnO<sub>2</sub> crystal at 310 h.

Fig.1a shows the time-series XRD patterns of SnO<sub>2</sub> QDs coarsened in 1.2 M NaOH solution at 250 °C. Narrowing X-ray diffraction profiles at 1.5 h indicates that, the growth of SnO<sub>2</sub> restarted basically right after a NaOH addition. By contrast, nano-SnO<sub>2</sub> can stabilize around 4-5 nm in water over 100 h in pure water as shown in our previous work.<sup>7</sup> Particle size calculation by using the Scherrer equation further demonstrates that, within 96 h (Table S1 and Fig.S1 in the Supporting Information), the average size of SnO<sub>2</sub> along [002] direction gradually increased to ~36.0 nm, whereas the evaluated size along vertical [110] direction basically stayed unchanged around 4-5 nm. It implies preferred orientation growth of SnO<sub>2</sub> nanocrystals. Remarkable change occurred at 240 and 310 h. A group of extremely narrow peaks related to tetragonal SnO<sub>2</sub> appeared (Fig.1b). The sharp peaks indicate that following preferred orientation growth of SnO<sub>2</sub>, big (bulk-like) crystals appeared.

The size and shape of SnO<sub>2</sub> after NaOH addition were verified by transmission electron microscopy (TEM) and scanning electron microscopy (SEM). As shown in Fig.2a, inset ring-like selected area electron diffraction (SAED) pattern implies random orientation of SnO<sub>2</sub> QDs, before treated in NaOH solution. After coarsened in NaOH solution for 1.5 h, SnO<sub>2</sub> QDs and nanorods with similar width (Fig.2b) coexisted. When the time came to 24 h, nanowires with preferred [11-2] direction appeared (Fig.2d). In line with XRD analysis, SEM (Fig.2e and Fig.S2) and TEM (Fig. 3e) images confirm the appearance of micron-sized SnO<sub>2</sub> crystals at 310 h: big elongated crystals with roughly 200 nm in diameter and over 1 μm in length. The bulk-like crystals comprised of aggregated nanobelts, roughly 200 nm in width and tens of nm in thickness (Fig.3f). A likely edge of a nanobelt on big crystal surface can also be found in enlarged SEM image (Fig.2e). SAED pattern of nanobelts aggregate was that of a single crystal (Fig.3f), demonstrating a precise arrangement of nanobelts with parallel crystallographic alignment. Apparently, as-formed big crystals show the textures of mesocrystals

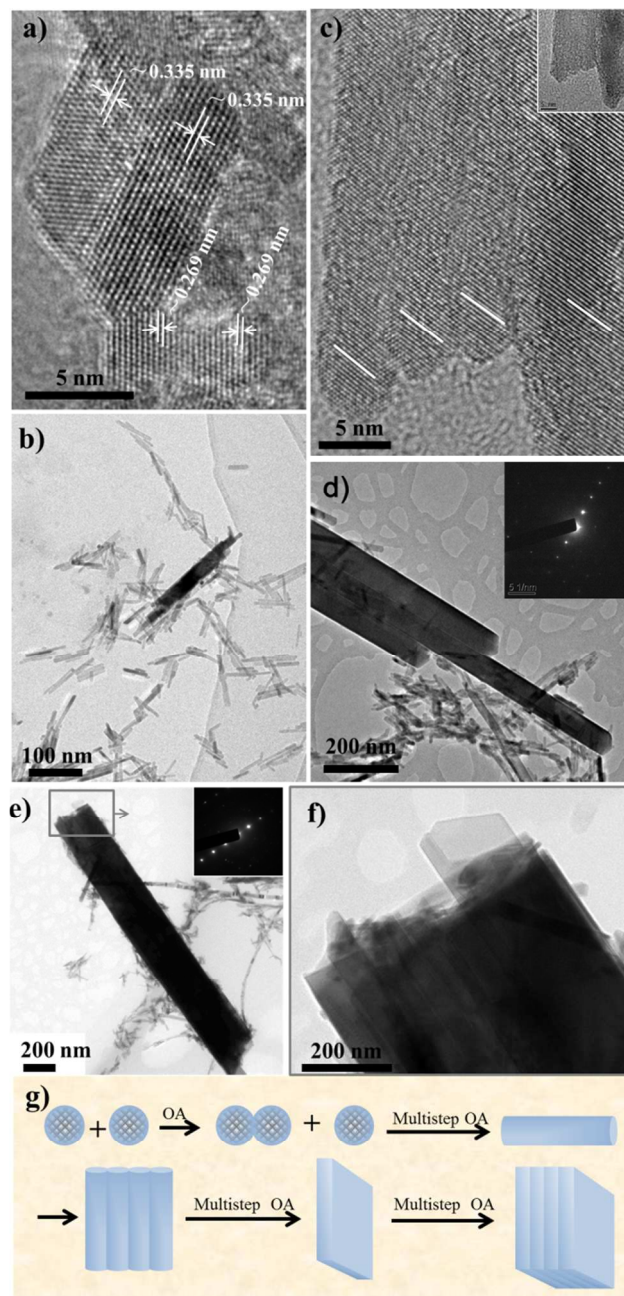


**Fig.3** TEM analysis of SnO<sub>2</sub> coarsened in 1.2 M NaOH at 250 °C: a) 1.5 h: attachment of two SnO<sub>2</sub> nanorods via side-by-side model. b-c) 240 h: side-by-side attachment and coalescence of adjacent nanowires. The white parallel lines in (c) highlight the common orientation. d-e) 310 h: parallel assembly of three micron-sized nanowires into a likely nanobelt, and parallel assembly of nanobelts into elongated micron crystal. Inset in d and e shows single-crystal-like diffraction pattern, indicating a common orientation of nanocrystals. f) HRTEM of crystal shown in e. g) Scheme illustrating a possible mechanism for nanowire formation via a multistep OA process and thereafter OA assembly of nanowires.

coined by Cölfen and Mann,<sup>21</sup> the formation of which are usually assisted by organic templates or additives. The above clues imply the self-assembly of SnO<sub>2</sub> QDs into hierarchically ordered nanostructures.

TEM analysis further describes the trace by which the hierarchically SnO<sub>2</sub> nanostructure formed. Firstly, as shown in Fig.2 a-d, a comparison of the size reflects that in initial stage, the width of nanorods or wires along [110] direction (around 4-5 nm) is close to

that of originally tiny QDs. The observation is in line with the XRD analysis that the average particle size along [110] direction basically stayed unchanged. TEM analysis further demonstrates that, several QDs with common crystallographic orientation collided and combined together to form nanowires (Fig.2e and Fig. S3). The clues demonstrate that the growth of SnO<sub>2</sub> was dominant by the OA mechanism. SAED pattern from an individual nanowire indicates that the obtained SnO<sub>2</sub> nanowire is a single crystal (Fig.2d). As described by Pacholski *et al.*,<sup>22</sup> the conventional OR (dissolution-reprecipitation) mechanism might assist to fill up the bottle-necks between two adjacent nanoparticles. The results imply that, after NaOH addition, a preferred oriented growth of SnO<sub>2</sub> QDs into nanowires could occur via a multistep OA growth route as illustrated in Fig.3f.

Besides the QDs, the large-sized SnO<sub>2</sub> crystals also shows the trace of OA-like growth. However, different from the QDs, the attachment of nanorods sometimes occurred via a side-by-side way (Fig.3a). The phenomenon of side-by-side attachment is more common among adjacent nanowires (Fig. 3b-c). As shown in Fig.3c, at 240 h, four SnO<sub>2</sub> nanowires attached with each other showing parallel crystallographic alignment. The perfect alignment of internal crystal lattices indicates a growth of parallel nanowires into a single crystal. When it came to 310 h, the parallel attachment and assembly of nanowires with width about 50 nanometers and length up to several hundred nanometers occurred (Fig.3d). Single-crystal-like SAED pattern confirms the same orientation of three big nanowires. As illustrated in Fig.3g, large-sized SnO<sub>2</sub> nanowire being “living” nanoparticle, grew via a multistep OA process, which help to describe the occurrence of SnO<sub>2</sub> nanobelts, the building blocks of hierarchical structure. As for small SnO<sub>2</sub> QDs and nanorods, the attachment of SnO<sub>2</sub> nanocrystals normally prefer on the high-energy surface along c axis (although it also happens along other crystal orientations sometimes). When the size of nanocrystals increases, the relative area of high-energy surface fast diminishes, and the probability of particles collision on high-energy surface reduces. In this case, the larger side area than cross-sectional area of nanowires, might facilitate the side-by-side attachment.

So far, real-time TEM imaging has indicated that the drift velocity of adjacent nanocrystals increases with the decrease interparticles distance.<sup>11, 12</sup> It has also been reported that, the presence of OH<sup>-</sup> is considered to possibly promote interfacial reactions through hydrogen bonds between adjacent particles,<sup>17, 18</sup> and neutralization of surface species by the hydrolytic transformation of hydroxy (OH<sup>-</sup>) centers to oxo (O) bridges releases protons that can reduce the surface charge of dispersed nanoparticles.<sup>21</sup> With these effects, it can thereby induce aggregation, reduce energy barrier, and bridge the OA-like growth of adjacent nanocrystals. The role of NaOH could also be a change of pH, that influences the growth behavior. We hope to do more efforts to find out some clues to the effects of NaOH in future.

In conclusion, taking SnO<sub>2</sub> QDs with random orientation as precursor, NaOH induces a continuously growth of QDs to nanowires, side-by-side attachment of which forms hierarchical ordered structures. OA growth can be dominant even in micron size, and in the later stages assembly stages of crystal growth. Coupled with our previous studies, we can find that the size, aggregation and surface treatment coordinately control the crystallization pathways of insoluble nanomaterials, leading to the formation of nanostructure ranging from polycrystalline,<sup>7</sup> single crystal,<sup>16</sup> and to mesocrystal in this work. In contrast to aggregation-induced steeply “jump of size” growth tendency,<sup>16</sup> an effective surface modification favoring the attachment and coalescence of adjacent nanocrystals, could possibly provide a moderate way for regulating crystal growth. The finding in

this work can show some guidances for biomimetic syntheses of complex nanomaterials with novel properties.

This work was supported by the National Basic Research Program of China (2010CB933501, 2013CB934302), the Outstanding Youth Fund (21125730), the National Science Foundation Grant (21273237, 51402295).

## Notes and references

<sup>a</sup> State Key Laboratory of Structures, Fujian Institute of Research on the Structure of Matter, Chinese Academy of Sciences, Fuzhou, Fujian, 350002, China.

Electronic Supplementary Information (ESI) available as noted in the text. See DOI: 10.1039/c000000x/

1. A. Verch, D. Gebauer, M. Antonietti and H. Colfen, *Phys Chem Chem Phys*, 2011, **13**, 16811-16820.
2. J. F. Banfield, S. A. Welch, H. Z. Zhang, T. T. Ebert and R. L. Penn, *Science*, 2000, **289**, 751-754.
3. J. Zhang, F. Huang and Z. Lin, *Nanoscale*, 2010, **2**, 18-34.
4. J. H. Zhan, H. P. Lin and C. Y. Mou, *Adv Mater*, 2003, **15**, 621-623.
5. H. Colfen and M. Antonietti, *Angew Chem Int Edit*, 2005, **44**, 5576-5591.
6. R. L. Penn and J. F. Banfield, *Science*, 1998, **281**, 969-971.
7. Z. Y. Zhuang, J. Zhang, F. Huang, Y. H. Wang and Z. Lin, *Phys Chem Chem Phys*, 2009, **11**, 8516-8521.
8. C. Ribeiro, E. J. H. Lee, E. Longo and E. R. Leite, *Chemphyschem*, 2005, **6**, 690-696.
9. M. Niederberger and H. Colfen, *Phys Chem Chem Phys*, 2006, **8**, 3271-3287.
10. Z. P. Zhang, H. P. Sun, X. Q. Shao, D. F. Li, H. D. Yu and M. Y. Han, *Adv Mater*, 2005, **17**, 42-47.
11. H. G. Liao, L. K. Cui, S. Whitelam and H. M. Zheng, *Science*, 2012, **336**, 1011-1014.
12. D. S. Li, M. H. Nielsen, J. R. I. Lee, C. Frandsen, J. F. Banfield and J. De Yoreo, *Science*, 2012, **336**, 1014-1018.
13. W. Tian, C. Zhang, T. Y. Zhai, S. L. Li, X. Wang, M. Y. Liao, K. Tsukagoshi, D. Golberg and Y. Bando, *Chem Commun*, 2013, **49**, 3739-3741.
14. H. B. Feng, J. Huang and J. H. Li, *Chem Commun*, 2013, **49**, 1017-1019.
15. E. R. Leite, T. R. Giraldo, F. M. Pontes, E. Longo, A. Beltran and J. Andres, *Appl Phys Lett*, 2003, **83**, 1566-1568.
16. Z. Y. Zhuang, F. Huang, Z. Lin and H. Z. Zhang, *J Am Chem Soc*, 2012, **134**, 16228-16234.
17. K. K. Sand, M. Yang, E. Makovicky, D. J. Cooke, T. Hassenkam, K. Bechgaard and S. L. S. Stipp, *Langmuir*, 2010, **26**, 15239-15247.
18. H. W. Wang, D. J. Wesolowski, T. E. Proffen, L. Vlcek, W. Wang, L. F. Allard, A. I. Kolesnikov, M. Feygenson, L. M. Anovitz and R. L. Paul, *J Am Chem Soc*, 2013, **135**, 6885-6895.
19. B. Cheng, J. M. Russell, W. S. Shi, L. Zhang and E. T. Samulski, *J Am Chem Soc*, 2004, **126**, 5972-5973.
20. C. Wang, Y. Zhou, M. Y. Ge, X. B. Xu, Z. L. Zhang and J. Z. Jiang, *J Am Chem Soc*, 2010, **132**, 46-47.
21. H. Colfen and S. Mann, *Angew Chem Int Edit*, 2003, **42**, 2350-2365.
22. C. Pacholski, A. Kornowski and H. Weller, *Angew Chem Int Edit*, 2002, **41**, 1188-1191.

TOC

